DEUTERON FLUCTUATIONS AND PROTON–DEUTERON CORRELATIONS FROM THE STAR EXPERIMENT AT $\sqrt{s_{NN}} = 7.7$–200 GeV*

Debasish Mallick

for the STAR Collaboration

National Institute of Science Education and Research, HBNI, Jatni-752050, India
dmallick@rcf.rhic.bnl.gov

*Received 1 August 2022, accepted 2 September 2022,
published online 14 December 2022*

The production mechanism of deuterons, which have a binding energy of 2.2 MeV, is a topic of current interest in high-energy heavy-ion collisions. Two of common scenarios are statistical thermal process and coalescence of nucleons. The cumulants of deuteron number and proton–deuteron correlations are sensitive to these physics processes. They are also sensitive to the choice of canonical *versus* grand canonical ensemble in statistical thermal models. We report on the first measurements of cumulant ratios (up to 4^{th} order) of the deuteron number and proton–deuteron correlations in Au+Au collisions at $\sqrt{s_{NN}} = 7.7$–200 GeV. Comparisons of the measurements to the thermal model calculations with a grand canonical, canonical ensemble, and the UrQMD model combined with a coalescence mechanism provide key insights into the mechanism of deuteron production in heavy-ion collisions.

DOI:10.5506/APhysPolBSupp.16.1-A80

1. Introduction

One of the primary goals of heavy-ion collision experiments is to study the phases of matter under extreme conditions such as temperature and/or pressure. High-energy heavy-ion collision experiments have established a new state of matter known as Quark–Gluon Plasma (QGP). Studying the particle-production mechanism in such collisions gives a direct opportunity to study this state of matter. The mean yields of hadrons as well as of light nuclei produced in central heavy-ion collisions can be explained within the thermal statistical model for suitable choices of chemical freeze-out parameters. The typical values of chemical freeze-out temperature (T) of the system

* Presented at the 29^{th} International Conference on Ultrarelativistic Nucleus–Nucleus Collisions: Quark Matter 2022, Kraków, Poland, 4–10 April, 2022.

created in such collisions vary from 140 to 155 MeV [1–3]. The puzzle on the light-nuclei production in these collisions naturally arises as their binding energies are of the order of only a few MeV, which is much lower than the freeze-out temperature of the medium. The other approach to understand the production of light nuclei is the coalescence mechanism, where light nuclei are formed by coalescing protons and neutrons close by in the phase space. This approach predicts the constituent nucleon number scaling [4] of the elliptic flow of light nuclei. Such a property has been observed in the STAR experiment [5].

Higher order cumulants have been extensively studied to understand the thermodynamics of the system. In particular, the higher order cumulants of event-by-event deuteron number distribution and proton–deuteron correlations are predicted to have distinct natures in the thermal and coalescence models [6]. Further, theoretical calculations suggest that the production of light nuclei might be affected by the presence of a QCD critical point and first-order phase transition due to their sensitivity to the local fluctuations in neutron density [7, 8]. As deuterons carry two baryons, their fluctuations will also enhance our understanding of baryon number fluctuation. In these proceedings, we report on the measurements of cumulant ratios of deuteron number distribution and proton–deuteron correlation for 0–5% and 70–80% centralities in Au+Au collisions for $\sqrt{s_{NN}} = 7.7$ to 200 GeV.

2. Analysis methods

Events of minimum-bias Au+Au collisions at $\sqrt{s_{NN}} = 7.7$, 11.5, 14.5, 19.6, 27, 39, 54.4, 62.4, and 200 GeV are analyzed for the measurement using the STAR detector at RHIC. Deuterons are identified using both Time Projection Chamber (TPC) and Time-of-Flight (TOF) detectors in the transverse momentum (p_{T}) range of 0.8 to 4 GeV/c and within mid-rapidity ($|y| < 0.5$). For the proton–deuteron correlation measurement, protons are identified in $|y| < 0.5$, using only TPC for $0.4 < p_{\mathrm{T}} < 0.8$ GeV/c, while both TPC and TOF detectors are used for the range of $0.8 < p_{\mathrm{T}} < 2.0$ GeV/c [9, 10]. The collision centrality is determined from the charged particle multiplicity (measured within $|\eta| < 1$) excluding the particles of interest (protons and deuterons) to avoid the auto-correlation effect. To suppress the effects of volume fluctuations, cumulants are calculated in each multiplicity bin and the centrality bin-width correction is applied [11]. Cumulants are also corrected for the finite detection efficiencies and acceptance effects with the assumption that the detector response is binomial in nature [12]. Statistical uncertainties are calculated using the bootstrap method [10, 13]. For the systematic uncertainty estimation, track quality, particle identification criteria, and detection efficiencies are varied within reasonable ranges.

3. Results

Figure 1 shows the event-by-event deuteron number distribution for the central 0–5% Au+Au collisions for $\sqrt{s_{NN}} = 7.7$, 39, and 200 GeV. Deuteron numbers shown are uncorrected for the detection efficiency. The mean and width, as can be seen from the distributions, increase as collision energy decreases. This trend can be understood from the fact that baryon chemical potential also increases towards lower $\sqrt{s_{NN}}$, resulting in enhanced production of deuterons.

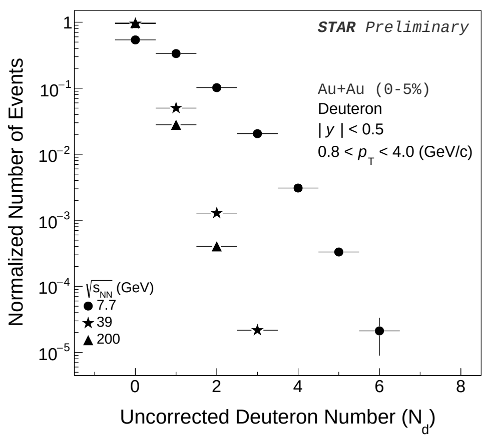

Fig. 1. Event-by-event deuteron number distribution for the central (0–5%) Au+Au collisions for $\sqrt{s_{NN}} = 7.7$, 39, and 200 GeV. Deuteron numbers are not corrected for efficiency.

Cumulants calculated from the deuteron distributions are corrected for the centrality bin-width effect and detection efficiencies. Figure 2 shows the deuteron $\kappa\sigma^2$, $S\sigma$, σ^2/M, and proton–deuteron correlation for the central 0–5% and peripheral 70–80% Au+Au collisions at $\sqrt{s_{NN}} = 7.7$ to 200 GeV. At higher $\sqrt{s_{NN}}$, the cumulant ratios in 0–5% centrality are close to the Poisson baseline (unity) and deviate from unity as $\sqrt{s_{NN}}$ decreases. In central collisions, they show smooth dependence on collision energy. The $\kappa\sigma^2$ shows the largest deviation from unity compared to the other two ratios which involve lower order cumulants. Suppression arises due to the global baryon number conservation, which affects the measurements performed at mid-rapidity. In central collisions at lower $\sqrt{s_{NN}}$, increased baryon stopping and acceptance covering a larger part of phase-space result in a more observable effect of baryon number conservation. Corresponding results in 70–80% peripheral centrality show weak dependence on $\sqrt{s_{NN}}$.

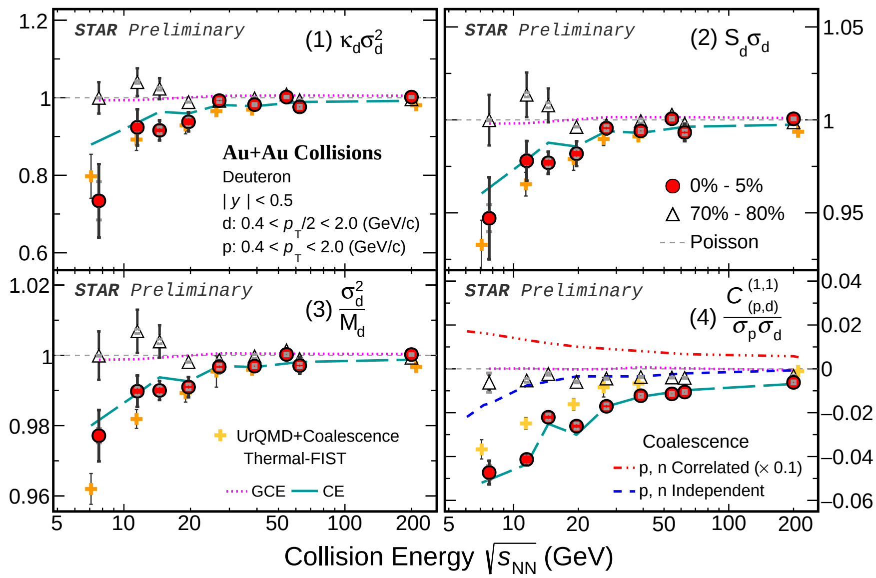

Fig. 2. (Color online) Cumulant ratios of deuteron distributions and proton–deuteron correlation shown as a function of collision energy. Red circle and open triangle markers represent measurements for most central (0–5%) and peripheral (70–80%) collisions, respectively. Bars and brackets symbols represent the statistical and systematic uncertainties, respectively. UrQMD+phase-space coalescence calculations are shown using orange cross markers. Thermal-FIST model calculations for GCE and CE are shown using magenta (dotted) and cyan (long-dashed) lines, respectively. In panel (4), results for correlated and independent proton (and neutron) distributions in the toy model simulation of the coalescence process from Ref. [6] are shown using red (triple-dot–dashed) and blue (dashed) lines, respectively.

The calculations for the thermal model with Grand Canonical Ensemble (GCE) and Canonical Ensemble (CE) are obtained from Thermal-FIST [14]. These calculations are performed for the central 0–5% collisions with experimental acceptances. The chemical freeze-out parameters published by the STAR experiment [1] from the fit of hadronic mean yields are used for the calculation. The CE Thermal-FIST model uses a volume called canonical correlation volume, V_c, over which the exact conservation of baryon number is implemented. The V_c parameter is varied at each $\sqrt{s_{NN}}$ for a reasonable agreement of model calculations with the measured cumulant ratios and Pearson's coefficient. The cyan-colored long-dashed lines represent results corresponding to minimum χ^2 obtained from the scan of parameter V_c to explain the cumulant ratios and proton–deuteron correlation. Measurements favour V_c parameter close to $4\mathrm{d}V/\mathrm{d}y$ at higher $\sqrt{s_{NN}}$, which decreases towards lower collision energies. For the condition $V_c \to \infty$, the measured part of the system approaches to GCE limit. The smaller values of V_c at lower collision energies imply the importance of baryon number conservation effect on the measurements.

For higher $\sqrt{s_{NN}}$, cumulant ratios in central 0–5% show reasonable agreement with both the GCE and CE thermal model expectations. However, GCE seems to fail to describe the ratios for $\sqrt{s_{NN}} \leq 20$ GeV. The CE thermal model predicts the suppression of cumulant ratios. The corresponding results for 0–5% Au+Au collisions from a UrQMD model, combined with a phase-space coalescence mechanism (with a hard cut on relative momentum and distance between protons and neutrons), also predict energy dependence trend of cumulant ratios.

Panel (4) of Fig. 2 shows that for all collision energies and centralities presented, the Pearson correlation coefficient between proton and deuteron number is negative. This anti-correlation becomes stronger for central collisions as $\sqrt{s_{NN}}$ decreases. Corresponding results for peripheral collisions do not show any $\sqrt{s_{NN}}$ dependence and are close to zero. The GCE thermal model fails to predict the anti-correlation. The CE thermal model correctly predicts the sign and $\sqrt{s_{NN}}$ dependence trend of the correlation. Results from the simple statistical simulation of the coalescence process from Ref. [6] are shown for central collisions for two assumptions on the proton and neutron number distributions. In one case, they are fully correlated (*i.e.* $N_p = N_n$, where N_p and N_n are proton and neutron numbers in one event, respectively) and in the other case, they are completely independent. Neither the correlated nor independent assumption for proton and neutron number reproduce the data. However, the UrQMD+coalescence model predicts the trend of the experimental data in the central 0–5% collisions. This suggests that the phase-space density information of constituent nucleons is important for the coalescence mechanism. The negative sign of the Pearson correlation coefficient suggests the importance of baryon number conservation in hadron–nuclei correlations.

4. Summary

We presented the cumulant ratios of deuteron number and proton–deuteron correlations for the central 0–5% and peripheral 70–80% Au+Au collisions at $\sqrt{s_{NN}} = 7.7$ to 200 GeV. Cumulant ratios at higher $\sqrt{s_{NN}}$ are close to Poisson baseline, unity, and are suppressed as the collision energy decreases. The GCE thermal model fails to describe the cumulant ratios below $\sqrt{s_{NN}} = 20$ GeV. The CE thermal model and the UrQMD model combined with a coalescence mechanism, both of which have the baryon number conservation implemented, correctly predict the suppression. We also observe that the Pearson correlation coefficient between proton and deuteron numbers is negative for all collision energies and centralities presented, and becomes even more negative for central 0–5% collisions as $\sqrt{s_{NN}}$ decreases. The GCE model fails to predict the sign of this correlation. However, both the CE thermal model and UrQMD+coalescence model correctly predict the sign and energy dependence trend of the experimental measurement.

We acknowledge the financial support by the Department of Atomic Energy, Government of India.

REFERENCES

[1] STAR Collaboration (L. Adamczyk *et al.*), *Phys. Rev. C* **96**, 044904 (2017).

[2] A. Andronic, P. Braun-Munzinger, K. Redlich, J. Stachel, *Nature* **561**, 321 (2018).

[3] STAR Collaboration (J. Adam *et al.*), *Phys. Rev. C* **99**, 064905 (2019).

[4] T.Z. Yan *et al.*, *Phys. Lett. B* **638**, 50 (2006).

[5] STAR Collaboration (L. Adamczyk *et al.*), *Phys. Rev. C* **94**, 034908 (2016).

[6] Z. Fecková, J. Steinheimer, B. Tomášik, M. Bleicher, *Phys. Rev. C* **93**, 054906 (2016).

[7] Kai-Jia Sun, Lie-Wen Chen, Che Ming Ko, Zhangbu Xu, *Phys. Lett. B* **774**, 103 (2017).

[8] E. Shuryak, J.M. Torres-Rincon, *Phys. Rev. C* **100**, 024903 (2019).

[9] STAR Collaboration (J. Adam *et al.*), *Phys. Rev. Lett.* **126**, 092301 (2021).

[10] STAR Collaboration (M. Abdallah *et al.*), *Phys. Rev. C* **104**, 024902 (2021).

[11] X. Luo, Ji Xu, B. Mohanty, N. Xu, *J. Phys. G: Nucl. Part. Phys.* **40**, 105104 (2013).

[12] T. Nonaka, M. Kitazawa, S. Esumi, *Phys. Rev. C* **95**, 064912 (2017); *Erratum ibid.* **103**, 029901 (2021).

[13] A. Pandav, D. Mallick, B. Mohanty, *Nucl. Phys. A* **991**, 121608 (2019).

[14] V. Vovchenko, H. Stoecker, *Comput. Phys. Commun.* **244**, 295 (2019).